

This is the Post-print version of the following article: *Lorena Delgadillo-Velasco, Virginia Hernández-Montoya, Norma A. Rangel-Vázquez, Francisco J. Cervantes, Miguel A. Montes-Morán, Ma. del Rosario Moreno-Virgen, Screening of commercial sorbents for the removal of phosphates from water and modeling by molecular simulation, Journal of Molecular Liquids, Volume 262, 2018, Pages 443-450*, which has been published in final form at: <https://doi.org/10.1016/j.molliq.2018.04.100>

© 2018. This manuscript version is made available under the Creative Commons Attribution-NonCommercial-NoDerivatives 4.0 International (CC BY-NC-ND 4.0) license <http://creativecommons.org/licenses/by-nc-nd/4.0/>

Accepted Manuscript

Screening of commercial sorbents for the removal of phosphates from water and modeling by molecular simulation

Lorena Delgadillo-Velasco, Virginia Hernández-Montoya, Norma A. Rangel-Vázquez, Francisco J. Cervantes, Miguel A. Montes-Morán, Ma del Rosario Moreno-Virgen



PII: S0167-7322(18)31563-0
DOI: doi:[10.1016/j.molliq.2018.04.100](https://doi.org/10.1016/j.molliq.2018.04.100)
Reference: MOLLIQ 9003
To appear in: *Journal of Molecular Liquids*
Received date: 23 March 2018
Revised date: 18 April 2018
Accepted date: 19 April 2018

Please cite this article as: Lorena Delgadillo-Velasco, Virginia Hernández-Montoya, Norma A. Rangel-Vázquez, Francisco J. Cervantes, Miguel A. Montes-Morán, Ma del Rosario Moreno-Virgen , Screening of commercial sorbents for the removal of phosphates from water and modeling by molecular simulation. The address for the corresponding author was captured as affiliation for all authors. Please check if appropriate. Molliq(2017), doi:[10.1016/j.molliq.2018.04.100](https://doi.org/10.1016/j.molliq.2018.04.100)

This is a PDF file of an unedited manuscript that has been accepted for publication. As a service to our customers we are providing this early version of the manuscript. The manuscript will undergo copyediting, typesetting, and review of the resulting proof before it is published in its final form. Please note that during the production process errors may be discovered which could affect the content, and all legal disclaimers that apply to the journal pertain.

Screening of commercial sorbents for the removal of phosphates from water and modeling by molecular simulation

Lorena Delgadillo-Velasco^a, Virginia Hernández-Montoya^{a,*}, Norma A. Rangel-Vázquez^a,
Francisco J. Cervantes^b, Miguel A. Montes-Morán^c, Ma del Rosario Moreno-Virgen^a

^aTecNM/Instituto Tecnológico de Aguascalientes, Av. Adolfo López Mateos No. 1801 Ote. C.P. 20256, Aguascalientes, Ags., México.

^bDivisión de Ciencias Ambientales, Instituto Potosino de Investigación Científica y Tecnológica (IPICYT), Camino a la Presa San José 2055, Col. Lomas 4^a. Sección, San Luis Potosí, SLP, 78216 México.

^cInstituto Nacional del Carbón, INCAR-CSIC, Apartado 73 E-33080, Oviedo, Spain.

Abstract

Eight commercial sorbents of different origin and nature were studied in the present work for the removal of phosphate from water using synthetic solutions and a wastewater from an anodizing company. The materials included activated carbons, bone char, catalytic carbon, natural silica, natural zeolite, a manganese(II) oxide composite and iron(III) hydroxide. These materials were characterized with different analytical techniques such as nitrogen adsorption isotherms at -196 °C, FT-IR spectroscopy, SEM/EDX analysis and X-ray diffraction. The adsorption studies were performed in batch systems. Iron(III) hydroxide was found the best sorbent, showing a maximum adsorption capacity of 193.75 mg/g at pH 7 in contrast with natural zeolite and silica, which registered very low adsorption values (2.92 and 4.17 mg/g, respectively). According to molecular simulation studies, the adsorption of phosphates from water on iron(III) hydroxide allowed the formation of the complex $\equiv\text{FePO}_4\text{H}_2$, with a Gibbs free energy of -21.38 kcal/mol, showing that it is possible to recover

*Corresponding author. Tel.: +52 449 9105002 Ext. 137

E-mail address: virginia.hernandez@yahoo.com.mx (Virginia Hernández-Montoya)

the phosphates and reuse them later. The adsorbed amount of phosphates on iron(III) hydroxide using synthetic solutions and the industrial wastewater was similar thus suggesting that iron(III) hydroxide is a selective sorbent for the removal of phosphates.

Keywords: Phosphates, sorbents, water, molecular simulation

1. Introduction

Phosphorus is one of the vital macronutrients for all living species and it is an element widely used in a variety of agricultural, industrial and everyday products [1]. Although phosphorus can be found naturally in the environment, frequently excessive amounts of phosphorus (usually in the form of phosphate) are present in water bodies by the discharge of untreated industrial wastewater and agricultural runoff [1-4]. The excessive concentration of phosphates has been linked to the degradation of water quality known as eutrophication [1-3, 5]. The principal effects of eutrophication are: the excessive growth of algae that reduce the transparency of water and whose decomposition when dying consumes the dissolved oxygen in the water, producing an unpleasant smell and the decrease of aquatic life [1-3, 5].

In Mexico, the permissible level of phosphorus in the water to prevent the effects of eutrophication is 0.05 mg/L [6]. To achieve this level, there are different treatment methods available for the removal of phosphate from wastewater. These methods are physical (reverse osmosis and electro-dialysis) [3], biological (conventional activated sludge process, anaerobic fermentation, biofilm reactors, sequentially combined aerobic and anaerobic batch reactors) [3, 7] and physico-chemical (chemical precipitation, crystallization, ligand exchange, adsorption, magnetic separation, nanotechnology) [1]. However, physical methods

are either considered expensive or ineffective in removal of phosphate [3, 8], whereas the biological methods are unstable due to their sensitivity to operation parameters such as: phosphate concentration and pH variations [7, 8]. Meanwhile, physico-chemical methods are more attractive, especially the adsorption method, which combines the possibility of recovering phosphorus [1-3] with a high effectiveness and easy operation [3-4,8-9]. Adsorption does not have the disadvantage of the large amounts of sludge generated by other methods such as chemical precipitation [3-4, 8]. In this context, the most commonly used adsorbents for the removal of phosphates from water are: natural materials (e.g., sand, limestone, clay minerals, zeolite, Fe-oxides/(oxy)hydroxides, palygorskite) and waste materials or by-products (e.g., fly ash, furnace steel slag, red mud, sugar wastes, sawdust, etc.) [1-5,9-10]. In particular, it is well known that adsorbents as Fe-oxides/(oxy) hydroxides have a good phosphate binding capacity [11]. They are economical, environmentally friendly, chemically stable and non-toxic [12]. For these reasons, the coating of different granular materials with Fe-oxides/(oxy) hydroxides has been proposed to increase their stability, surface area, adsorption capacity and to facilitate the recovery of phosphates [11]. In this context, there are studies that focus on the modification and synthesis of new adsorbents to improve phosphate removal by adsorption. Some of these materials are: organic/amino functionalized mesoporous silica, metal-doped silica, mesoporous metal oxide/hydroxide [3], sulphate-coated zeolite/hydrotalcite/activated alumina [2], MgO impregnated biochar [3,7], iron-modified biochars [3, 8, 13], MnO₂ [14], rice husk and fruit juice residue based biochars [15], carboxymethylated sugarcane bagasse fibers incorporating Fe²⁺ ions [16], La(III)/Mg(OH)₂ modified bentonite [17], acid-activated neutralized red mud [9], magnetic biosorbents [13, 5] and others.

On the other hand, two of the most influential operational parameters for the adsorption of phosphates are: the initial concentration and the pH of aqueous solution [1, 3-4, 7-9, 12-13, 15, 17]. At the same time, most phosphate removal studies focus on the removal of phosphate from synthetic solutions using low concentrations (≤ 100 mg/L) [7, 11, 13, 15-18]; only a few of them test their adsorbents with phosphate solutions of high concentrations (> 100 mg/L) [2, 8, 9] or real wastewaters [7, 12].

In Mexico, the automotive industry has experienced a massive development in recent years [19, 20]; accounting for the second most important activity within the manufacturing sector (18.5 percent of México's manufacturing industry in 2015) [20]. Closely linked to the automotive industry is the coating and finishing of metal products industry [20], which generally includes different coating processes such as electroplating and electroless plating. These are multistep procedures (e.g., washing, pickling, cleaning, electrolytic baths, plating steps, post-treatments and rinsing) that consume a large amount of water and various chemical products (e.g. phosphoric acid) [21, 22]. The wastewater of these industries is normally a complex mixture of different dissolved pollutants (such as phosphate, heavy metals, dyes, etc.) which are difficult to treat. For this reason, cleaning these wastewaters comprises sequential stages for the removal of different water contaminants. Specifically, the removal of phosphates by adsorption can be considered as a tertiary treatment in typical treatment plants. In this context, the aim of this study is to compare the removal of phosphates from water using different commercial sorbents available in the Mexican market. The sorbents were tested in standard phosphate solutions and a wastewater collected from an anodizing industry located in Aguascalientes (Mexico). In addition, the sorbents studied in this work were characterized by different analytical techniques and the adsorption

mechanism of the material showing the highest phosphate removal capacity was studied by molecular simulation.

2. Materials and methods

2.1 Sorbents

Eight commercial sorbents were studied in this work including carbon and inorganic materials such as: 1) coconut shell activated carbon (CC), 2) bituminous coal activated carbon (B), 3) bone char (BC), 4) natural zeolite (Z), 5) silica (S), 6) Ferrolox (F), 7) Catalytic Carbon (CtC) and 8) Katalox light (KL). The general characteristic and specifications provided by the supplier are listed in Table 1. All the sorbents were first milled and sieved using the U.S.A. Standard Testing Sieves No. 30-25 (0.5-0.85 mm); then, the materials were rinsed several times with deionized water (30 °C, 5-150 rpm) until constant pH, to remove impurities. Finally, the sorbents were dried at 110 °C during 24 h and stored in plastic jars for later use.

2.2. Phosphate adsorption studies

The adsorption studies of phosphates were performed in batch systems with constant agitation (150 rpm) under the following experimental conditions: 30 °C, mass to volume ratio of 2 g/L, pH 2 and 7 (adjusted with 1M NaOH or 1M HCl) and equilibrium time 72 h (data obtained from adsorption kinetic studies which are not presented in this work). Two types of water were used in the present work, the first was a synthetic solution prepared with NaH₂PO₄ [Sigma-Aldrich, CAS Number 7558-80-7]) and deionized water (Milli-Q); and the second

type was wastewater collected from an anodized company located in Aguascalientes state (Mexico).

Three types of adsorption tests were carried out, the first one was performed using synthetic solutions of phosphates of 500 and 1500 mg/L and all the sorbents considered in the present work. The second one included the equilibrium studies (adsorption isotherms) of the more efficient sorbents as identified in the previous test. The phosphate adsorption isotherms were measured at 30 °C using synthetic solutions with phosphate concentrations ranging from 10 to 5000 mg/L, at pH 2 and 7.

Finally, three samples of wastewater from an anodized industry were collected at different times of the year. The general characteristics of these samples of wastewater are cited in Table 2. Particularly, the sample with the highest concentration of phosphates (5069 mg/L) was selected to perform the third type of adsorption test under adsorption conditions as mentioned above (batch reactor using constant stirring, 30 °C and mass to volume ratio of 2 g/L, 72 h equilibrium time).

Phosphate concentration in all the experiments was determined by the colorimetric method 8114 (Molybdovanadate method) of the standard HACH methods, using a HACH DR-5000 spectrophotometer.

2.3 Characterization of the sorbents

The eight sorbents studied were characterized using different analytical techniques. The main textural parameters were calculated from their nitrogen adsorption isotherms at -196 °C measured in an automatic Micromeritics ASAP 2020 analyzer. Prior to the measurements,

the samples were outgassed overnight at 300 °C under vacuum for 8 h. The specific surface area was calculated using the Brunauer–Emmett–Teller (BET) model using the 0.05–0.3 relative pressure (p/p_0) interval. The total pore volume was determined from the amount of nitrogen adsorbed at a relative pressure of ~ 0.99 ; the micropore volume was obtained by applying the Dubinin-Raduskevich method. The functional groups of the eight sorbents were determined by FT-IR spectroscopy using a Thermo Scientific Nicolet iS10 spectrometer.

For the best performing materials in phosphate adsorption, the morphology and surface composition were studied by SEM/EDX analyses using a FE-SEM system Quanta FEG 650, FEI. Solid particles were dispersed on a graphite adhesive tab placed on an aluminum stub and no further coating was required. Also, the crystalline phases of these sorbents were analyzed by X-ray diffraction and their diffraction patterns were recorded in a Bruker D8 Advance diffractometer equipped with a Cu $K\alpha$ X-ray source operated at 40 kV and 40 mA. A single Göbel mirror configuration was used to monochromatize and focus X-rays on samples, attaining highly efficient parallel beam geometry. Diffraction data were collected by step scanning with a step size of $0.02^\circ 2\theta$ and a scan step time of 5 s.

2.4 Adsorption mechanism by molecular simulation

Molecular analysis was carried out using the HyperChem 8 software with the purpose to elucidate the adsorption mechanism of phosphates from water when using the most efficient sorbent. The structure of the different molecules was drawn using the default element option. Bond distances and angles were then optimized using the Model option of the HyperChem software. The structures were studied using an AMBER/ZINDO-1 hybrid model to determine

energy minimization and geometry optimization. Geometrical optimization was performed in vacuum employing the Polak-Ribiere algorithm and root mean square (RMS) of 0.001 kcal/Å mol was reached. QSAR properties were calculated also using Hyperchem software. All calculations were carried out on a DELL i7 computer.

3. Results and discussion

3.1 Adsorption of phosphates from synthetic solutions

The phosphates adsorption results from water of the eight commercial sorbents using synthetic solutions with different initial concentration (500 and 1500 mgPO₄⁻³/L) are shown in Fig. 1. Sorbents F (iron(III) hydroxide) and KL (clinoptilolite with MnO₂ coating) were the most efficient materials for the removal of phosphates from water, in terms of adsorption capacity. Also, the adsorbed amount of phosphates increased for some of the materials as the initial concentration increased from 500 to 1500 mg/L at pH 7. Particularly, the adsorbed amount on F increased from 76.04 to 128.75 mg/g and on KL from 23.54 to 30 mg/g. In this context, with the purpose to estimate the maximum adsorption capacity of F and KL, phosphate adsorption isotherms at 30 °C and pH 2 and pH 7 were obtained (Fig. 2). These conditions were selected based on the wastewater temperature and pH sampling variation (See Table 2). 30 °C is slightly above the maximum temperature of wastewater sampling (28 °C) and it is thus a confident value to estimate the adsorption capacity of the sorbents under the worst adsorption conditions. Data of Fig. 2a confirm that F (iron(III) hydroxide) has a higher adsorption capacity (194 mg/g at pH 7 and 323 mg/g at pH 2) than the KL sorbent (41 mg/g at pH 7 and 23 mg/g at pH 2). The effect of pH on the adsorption of both sorbents is contrasting, with F adsorbing more quantities at pH 2 and KL at pH 7. The maximum

adsorption capacity of phosphates on F at pH 2 (323 mg/g) is higher than the data reported for other materials as the goethite (5.69 mg/g) or comparable to composite of activated carbon fiber with iron hydroxide at the same pH (306 mg/g) [23-24].

With the purpose of elucidating the adsorption mechanism of phosphates on F, molecular analysis was carried out using the software HyperChem 8. Table 3 shows the QSAR properties of the iron(III) hydroxide (model compound and principal component of F) and NaH_2PO_4 (chemical reagent used in the preparation of standard solutions). The surface area, volume and mass are very similar for $\text{Fe}(\text{OH})_3$ and NaH_2PO_4 . However, a slight difference was observed in the molecular electrostatic potential (MESP) of these compounds, which are closely related to their electronic density distributions (Fig. 3). Red color means regions with the most negative electrostatic potential (EP), whereas blue color denotes regions where EP is most positive, and green corresponds to regions with zero potential. As expected, the reddest spots of the MESP maps are located on electronegative atoms such as O.

On the other hand, considering the information provided by the supplier and the results of the sorbent characterization (see below), F is a composite material (patented) containing other elements in its structure such as C, Mg, Si, Ca and Mn (See section 3.2). For this reason, it is not possible to establish an exact adsorption mechanism, but according to the data reported in the literature the adsorption of phosphates on iron(III) hydroxide is higher at low pH and at this condition is possible the formation of the surface complex $\equiv\text{FePO}_4\text{H}_2$ [23]. In this context, the interaction of $\text{Fe}(\text{OH})_3$ with NaH_2PO_4 in aqueous solution at low pH was simulated and the results indicated that the $\equiv\text{FePO}_4\text{H}_2$ complex is formed by the reaction shown in Fig. 4.

The QSAR properties of the complex in aqueous solution is shown in Table 3 and according to the value of Gibbs Free Energy (-21.38 kcal/mol), the formation of the complex is thermodynamically feasible, and the reaction is spontaneous. Also, the molecular electrostatic potential (MESP) of this complex evidence that in general, the electronic density decreases in comparison with the sorbent F and the adsorbate (NaH_2PO_4), as some green regions corresponding to zero potential are observed (See Fig. 3c).

3.2 Characterization of the sorbents

The textural parameters and organic functional groups of all sorbents considered in this work were determined from nitrogen adsorption isotherms at $-196\text{ }^\circ\text{C}$ and FT-IR spectroscopy, respectively. Fig. 5 shows the nitrogen adsorption isotherms at $-196\text{ }^\circ\text{C}$ and, according to the IUPAC classification, the isotherms of the CC, B and CtC are type I, which are characteristic of microporous materials; the isotherms of the BC, Z, F and KL sorbents are type IV(a), which is typical of mesoporous materials and finally, the isotherm of the S material is type II (nonporous materials). Table 4 summarize the principal textural parameters of all sorbents which were calculated using the appropriated models (see section 2.3). The activated carbons (CC, B and CtC) are the sorbents with the highest BET surface area (731, 818 and $810\text{ m}^2/\text{g}$, respectively). However, in general, the adsorption of phosphate from water was found to be higher on mesoporous materials (F, KL and BC) (See Fig. 1).

Fig. 6 shows the FT-IR spectra of the sorbents studied in this work. The different chemical functionalities are related to the origin of each sorbent. For example, the peak at 1015 cm^{-1} of inorganic sorbents such as KL (clinoptilolite- MnO_2), S (silica) and Z (natural

zeolite) is assigned to the stretching vibration Si-O of silanol groups [26] and the peak at $\sim 1630\text{ cm}^{-1}$ is due to the H-O-H bending vibration of adsorbed water in the inorganic structures [27]. For the activated carbons, i.e., CC (coconut shell activated carbon), B (bituminous coal activated carbon) and CtC (Coconut shell activated carbon coated with iron), three principal peaks are observed in the FT-IR spectra at 2927, 1518 and 1034 cm^{-1} , which are characteristics of C-H, C=C and C-O stretching vibrations, respectively [28]. Also, for BC (bone char), the characteristic peaks of hydroxyapatite (principal component of bone char) are evident at 1024, 1463 and 3375 cm^{-1} , which are assigned to the groups PO_4^{3-} , CO_3^{2-} and OH^- [29].

Finally, for the F (iron(III) hydroxide) sorbent the principal groups identified in the FT-IR spectrum are assigned to hydroxyl groups and the peaks located at 3385 and 1647 cm^{-1} are assigned to O-H stretching vibration and H-O-H bending vibration [30]. Also, considering that this sorbent F was the most efficient in the removal of phosphates from water, the elemental composition and morphology was analyzed by SEM/EDX and the crystalline structure by X-ray diffraction. Table 5 shows the elemental composition of F. Fe (33.91 %) and O (44.67 %) are the principal components of F and other elements such as Mg, Si, Ca and Mn are present in lower quantities. Additionally, Fig. 7 shows the SEM images of F granules at two magnifications. XRD analysis indicated that, despite the relatively high background of the diffraction pattern, the iron(III) hydroxide material used as sorbent is essentially amorphous (See Fig. S1 in supporting information).

3.3 Adsorption of phosphate from wastewater

The adsorption of phosphates from wastewater was studied on F and KL sorbents. As mentioned in the experimental section, only the wastewater sample containing the highest concentration of phosphates (5069 mg/L, Table 2) was used for this study. The adsorption results are shown in Fig. 8. The adsorbed amounts of phosphate from wastewater were 310.42 and 14.58 mg/g for F and KL, respectively. Also, in Fig. 8 are shown the adsorption results of F and KL when using a synthetic solution of phosphates of the same concentration (5069 mg/L) that was prepared by dissolving analytical grade NaH_2PO_4 in deionized water to determine the possible effects of other components present in the wastewater. The comparison of the adsorption results pointed out that the adsorption of phosphates decreased only 5% for the iron(III) hydroxide (sorbent F) and 49 % for KL. These results proof not only the high capacity of F for phosphates from water but also its high selectivity.

3. Conclusions

The results obtained in the present work show that the adsorption of phosphates on commercial sorbents follows the following trend: iron(III) hydroxide > manganese(II) oxide composite > bone char > activated carbon > silica and zeolite. Particularly, the adsorption of phosphates on iron(III) hydroxide (F) at low pH was controlled by the formation of the $\equiv\text{FePO}_4\text{H}_2$ complex, which according to molecular simulation would be formed spontaneously. In this context, the porosity of the sorbents was not limiting the adsorption of phosphates from water. The specific composition of the sorbents was more determinant. The maximum adsorption capacity of the F (iron(III) hydroxide) sorbent was higher at low pH

(300 mg/g) and this value is comparable to other materials containing iron compounds. Additionally, F showed a great selectivity for phosphates as demonstrated by its almost unaltered adsorption capacity when using either synthetic water or real wastewater.

ACKNOWLEDGEMENTS

This work was supported by CONACyT (project AGS-2012-C02-198207) and PCTI-Asturias/FEDER (EU) (GRUPIN14-117) project. MC. Delgadillo-Velasco acknowledges the grant (467325) received from CONACYT.

References

- [1] Y. Gong, D. Zhao, Physical–chemical processes for phosphorus removal and recovery, *Compr. Water Qual. Purif.* 3 (2014) 196-222.
- [2] W. Choi, S.Y. Lee, S.H. Lee, J.E. Kim, K.Y. Park, D.J. Kim, S.W. Hong, Comparison of surface-modified adsorbents for phosphate removal in water, *Water Air Soil Pollut.* 223 (2012) 2881–2890.
- [3] W. Huang, Y. Zhang, D. Li, Adsorptive removal of phosphate from water using mesoporous materials: A review, *J. Environ. Manage.* 193 (2017) 470-482.
- [4] M. Shams, M.H. Dehghani, R. Nabizadeh, A. Mesdaghinia, M. Alimohammadi, A.A. Najafpoor, Adsorption of phosphorus from aqueous solution by cubic zeolitic imidazolate framework-8: Modeling, mechanical agitation versus sonication, *J. Mol. Liq.* 224 A (2016) 151-157.

- [5] X. Xu, B. Gao, B. Jin, Q. Yue, Removal of anionic pollutants from liquids by biomass materials: A review, *J. Mol. Liq.* 215 (2016) 565–595.
- [6] DIARIO OFICIAL DE LA FEDERACIÓN, ACUERDO por el que se establecen los Criterios Ecológicos de Calidad del Aguas CE-CCA-001/89.
- [7] R. Li, J.J. Wang, B. Zhou, Z. Zhang, S. Liu, S. Lei, R. Xiao, Simultaneous capture removal of phosphate, ammonium and organic substances by MgO impregnated biochar and its potential use in swine wastewater treatment, *J. Cleaner Prod.* 147 (2017) 96-107.
- [8] Q. Yang, X. Wang, W. Luo, J. Sun, Q. Xu, F. Chen, J. Zhao, S. Wang, F. Yao, D. Wang, X. Li, G. Zeng, Effectiveness and mechanisms of phosphate adsorption on iron-modified biochars derived from waste activated sludge, *Bioresour. Technol.* 247 (2018) 537–544.
- [9] J. Ye, X. Cong, P. Zang, G. Zeng, E. Hoffmann, Y. Wu, H. Zang, W. Fang, Operational parameter impact and back propagation artificial neural network modeling for phosphate adsorption onto acid-activated neutralized red mud, *J. Mol. Liq.* 216 (2016) 35–41.
- [10] I. Anastopoulos, A. Bhatnagar, B.H. Hameed, Y.S. Ok, M. Omirou, A review on waste-derived adsorbents from sugar industry for pollutant removal in water and wastewater, *J. Mol. Liq.* 240 (2017) 179–188.
- [11] P.S. Kumar, T. Prot, L. Korving, K.J. Keesmn, I. Dugulan, M.C.M. Van Loosdrecht, G. Witkamp, Effect of pore size distribution on iron oxide coated granular activated

- carbons for phosphate adsorption – Importance of mesopores, *Chem. Eng. J.* 326 (2017) 231–239.
- [12] M. Li, J. Liu, Y. Xu, Q. Guangren, Phosphate adsorption on metal oxides and metal hydroxides: A comparative review, *Environ. Rev.* 24(3) (2016) 319-332.
- [13] J. Kyung-Wong, L. Soonjae, J.L. Young, Synthesis of novel magnesium ferrite (MgFe_2O_4)/biochar magnetic composites and its adsorption behavior for phosphate in aqueous solutions, *Bioresour. Technol.* 245 (2017) 751–759.
- [14] W. Yao, F.J. Millero, Adsorption of phosphate on manganese dioxide in seawater, *Environ. Sci. Technol.* 30 (1996) 536-541.
- [15] D. Yadav, M. Kapur, P. Kumar, M.K. Mondal, Adsorptive removal of phosphate from aqueous solution using rice husk and fruit juice residue, *Process Saf. Environ. Prot.* 94 (2015) 402-409.
- [16] W.S. Carvalho, D.F. Martins, F.R. Gomes, I.R. Leite, L.G. da Silva, R. Ruggiero, E.M. Richter, Phosphate adsorption on chemically modified sugarcane bagasse fibers, *Biomass and bioenergy* 35 (2011) 3913-3919.
- [17] S. Pandey, A comprehensive review on recent developments in bentonite-based materials used as adsorbents for wastewater treatment, *J. Mol. Liq.* 241 (2017) 1091-1113.
- [18] Y. Zhan, H. Zhang, J. Lin, Z. Zhang, J. Gao, Role of zeolite's exchangeable cations in phosphate adsorption onto zirconium-modified zeolite, *J. Mol. Liq.* 243 (2017) 624-637.

- [19] Barrera-Franco, A., Pulido-Morán, A., (2016), *La industria automotriz mexicana: situación actual, retos y oportunidades*, Ciudad de México, México, ProMéxico.
- [20] Instituto Nacional de Estadística y Geografía (INEGI) (2016), Statistics in occasion of... The Automotive industry. Aguascalientes, México. Recovered from: <http://www.amia.com.mx/>. REVISAR
- [21] A. Yli-Pentti, 4.11 – Electroplating and Electroless Plating, *Compr. Mater. Process.* 4 (2014) 277–306.
- [22] A. Agrawal, K.K. Sahu, An overview of the recovery of acid from spent acidic solutions from steel and electroplating industries, *J. Hazard. Mater.* 171 (2009) 61–75.
- [23] L. Zhang, Y. Gao, Y. Xu, J. Liu, Different performances and mechanisms of phosphate adsorption onto metal oxides and metal hydroxides: a comparative study, *J. Chem. Technol. Biotechnol.* 91 (2016) 1232–1239.
- [24] Z. Hongshao, R. Stanforth, Competitive adsorption of phosphate and arsenate on goethite, *Environ. Sci. Technol.* 35 (2001) 4753-4757.
- [25] A. Sperlich, Phosphate adsorption onto granular iron(III) hydroxide (gfh) for wastewater reuse, Doctoral Thesis, Berlin, 2010, pp. 1-111.
- [26] P.S. De Velasco-Maldonado, V. Hernandez-Montoya, M.A. Montes-Morán, N.A. Rangel-Vázquez, M.A. Pérez-Cruz, Surface modification of a natural zeolite by treatment with cold oxygen plasma: Characterization and application in water treatment, *Appl. Surf. Sci.* 434 (2018) 1193–1199.

- [27] F. Pechar, D. Rykl, Infrared spectra of natural zeolites of the stilbite group, Chem. zvesti 35 (1981) 189—202.
- [28] K.A. Krishnan, A. Haridas, Removal of phosphate from aqueous solutions and sewage using natural and surface modified coir pith, J. Hazard. Mater. 152 (2008) 527–535.
- [29] C.K. Rojas-Mayorga, A. Bonilla-Petriciolet, I.A. Aguayo-Villarreal, V. Hernández-Montoya, M.R. Moreno-Virgen, R. Tovar-Gómez, M.A. Montes-Morán, Optimization of pyrolysis conditions and adsorption properties of bone char for fluoride removal from water, J Anal. Appl. Pyrol. 104 (2013) 10–18.
- [30] S. Mustafa, M. Irshad, M. Waseem, K.H. Shah, U. Rashid, W. Rehman, Adsorption of heavy metal ions in ternary systems onto $\text{Fe}(\text{OH})_3$, Korean J. Chem. Eng. 30 (2013) 2235-2240.

Captions

- Fig. 1 Sorption results of the eight commercial sorbents using phosphate solutions of (a) 500 mg/L and (b) 1500 mg/L at pH 7, 30 °C and mass to volume ratio of 2 g/L.
- Fig. 2 Phosphate adsorption isotherms of the sorbents (a) F and (b) KL at pH 2 and pH 7. Experimental conditions: 30°, mass to volume ratio of 2 g/L, equilibrium time 72 h.
- Fig. 3 Comparison of the molecular electrostatic potential (MEP) 3D maps of (a) FeOH₃ (b) NaH₂PO₄ and (c) Complex NaH₂PO₄- Fe(OH)₃- H₂O.
- Fig. 4 Diagram of the reaction between NaH₂PO₄ and FeOH₃ during adsorption process
- Fig. 5 Sorption isotherms of nitrogen at -196 °C on the commercial adsorbents studied in the present work.
- Fig. 6 FT-IR spectra of the commercial sorbents studied in the present work
- Fig. 7 SEM images of the commercial F (iron(III) hydroxide) sorbent
- Fig. 8 Removal of phosphates using standard solutions and wastewater from anodized industry at the same experimental conditions: 30°, pH:1.86 mass to volume ratio of 2 g/L.

Table 1. Supplier specifications of the commercial adsorbents used for the removal of phosphate from water

Sorbent	Code	Origen or Nature	Property			Supplier
			Particle size (mm)	Specific surface area (m ² /g)	pH	
Coconut Shell activated carbon	CC	Vegetal. Thermal activation.	2.38-0.595	1050	7-8	Carbones Mexicanos Company
Bituminous coal activated carbon	B	Mineral. Thermal activation.	2.38-0.595	1000	8	Carbones Mexicanos Company
Bone char	BC	Animal: bovine bones	2.38-0.595	104	8-9.5	Carbones Mexicanos Company
Zeolite	Z	Natural Zeolite	1.18	25	8.91	Carbotecnia Company
Silica	S	Natural Silica	3.175-1.58	-	8.69	Carbotecnia Company
Ferrolox	F	Patented granular Iron hydroxide (70-85%)	1.5-4.0	270	7.71	Watch Water México Company
Catalytic Carbon	CtC	Coconut shell activated carbon (85%) with iron catalytic coating (FeO(OH) 15%)	2.4-0.6	2000-2500	9.5	Watch Water México Company
Katalox Light	KL	ZEOSORB (clinoptilolite [85%]) with a MnO ₂ coating (10%) and Ca(OH) ₂ (5%)	1.4-0.6	-	11.13	Watch Water México Company

Table 2. Characteristic of wastewater from the anodizing company

Parameter	Average of three quantifications		
	Sampling 1	Sampling 2	Sampling 3
Temperature, °C	28	16	27
pH	6.59	5.71	1.86
Phosphate concentration, mg/L	620	3240	5069

Table 3. QSAR properties of sorbate (NaH_2PO_4) and the sorbent denominated F ($\text{Fe}(\text{OH})_3$)


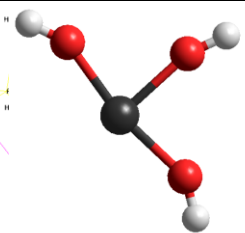

Property	NaH_2PO_4	$\text{Fe}(\text{OH})_3$	Complex $\text{Fe}(\text{OH})_3\text{-H}_2\text{O}$	$\text{NaH}_2\text{PO}_4\text{-}$
Molecule				
Surface Area (\AA^2)	213.13	209.90	644.96	
Volume (\AA^3)	274.08	242.32	1174.50	
Log P	0.57	0.48	-11.55	
Mass (amu)	119.98	106.87	587.15	
Gibbs free energy (kcal/mol)	0.3654	-0.022	-21.3887	

Table 4. Textural parameters of commercial sorbents, calculated from adsorption isotherms of N₂ at -196 °C, and the IUPAC classification.

Sorbent	^a S _{BET} , m ² /g	^b V _t , cm ³ /g	^c V _{mic} , cm ³ /g	IUPAC Classification	
				Type	Structure
CC	731	0.4750	0.3700	I	Microporous
B	818	0.5196	0.3974	I	Microporous
BC	64.6	0.098	0.029	IV (a)	Mesoporous
Z	27	0.064	0.0168	IV(a)	Mesoporous
S	< 5	0.0018	0.0014	II	Nonporous
F	233	0.5824	0.1043	IV(a)	Mesoporous
CtC	810	0.4428	0.4235	I	Microporous
KL	26	0.0958	0.0117	IV(a)	Mesoporous

a S_{BET}: BET surface area.

b V_t: Total pore volume.

c V_{mic}: Micropore volume.

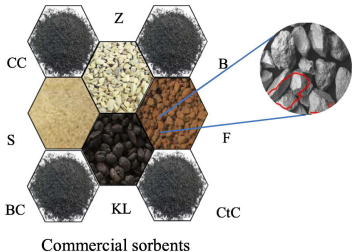
Table 5. Elemental composition of the F (ferric hydroxide) adsorbent as measured by EDX analysis

Element	Average of three quantifications (Wt %)	Standard deviation
C	5.46	0.42
O	44.67	5.64
Mg	1.18	0.06
Si	7.82	0.38
Ca	5.17	0.11
Mn	1.78	0.08
Fe	33.91	5.89

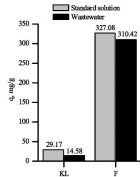
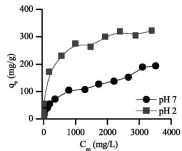
Highlights

- ▶ Commercial adsorbents are used in the removal of phosphates from synthetic solutions and wastewater
- ▶ The adsorbents include activated carbons, zeolites, silica and ferric hydroxide
- ▶ The chemical nature controls the adsorption capacity of the adsorbents, rather than their porosity
- ▶ Ferric hydroxide is the most efficient adsorbent for the removal of phosphates
- ▶ The complex $\equiv\text{FePO}_4\text{H}_2$ is formed during the adsorption of phosphates on ferric hydroxide.

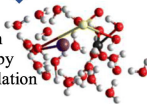
Phosphate water pollution



Phosphate sorption studies



Adsorption mechanism by molecular simulation



Graphics Abstract

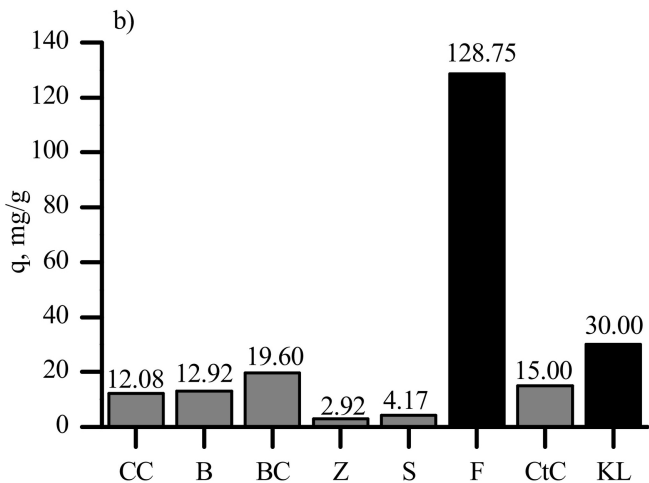
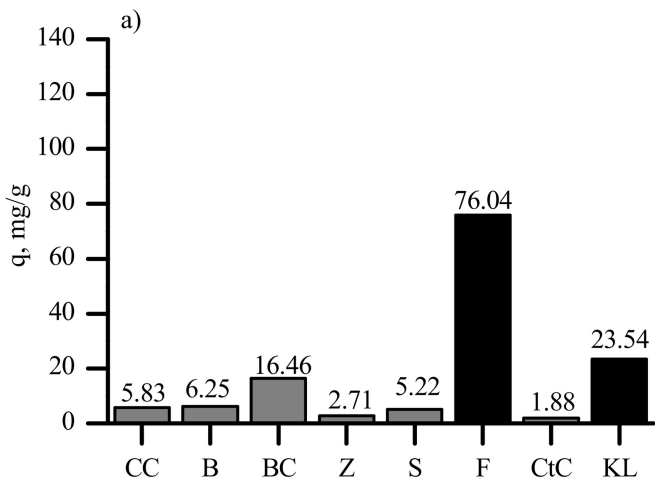


Figure 1

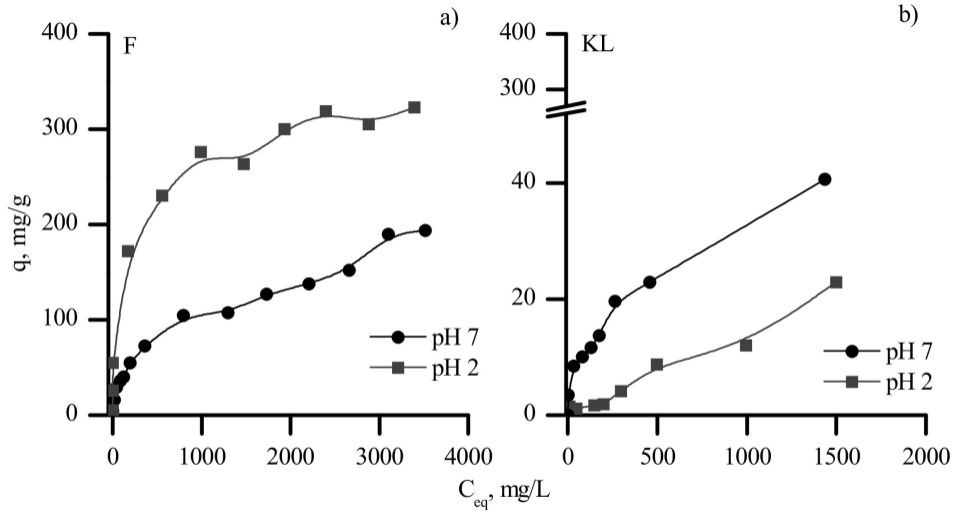
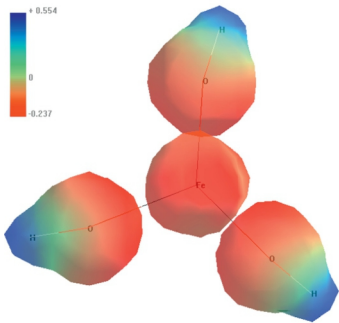
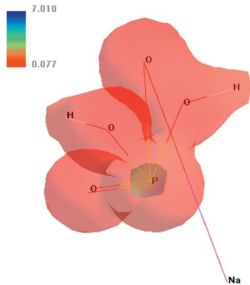


Figure 2

b) FeOH_3



a) NaH_2PO_4



c) Complex $\text{NaH}_2\text{PO}_4\text{-Fe(OH)}_3\text{-H}_2\text{O}$

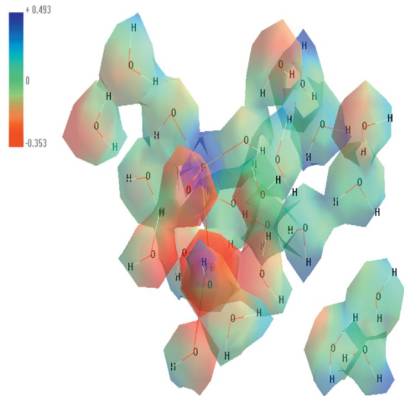


Figure 3

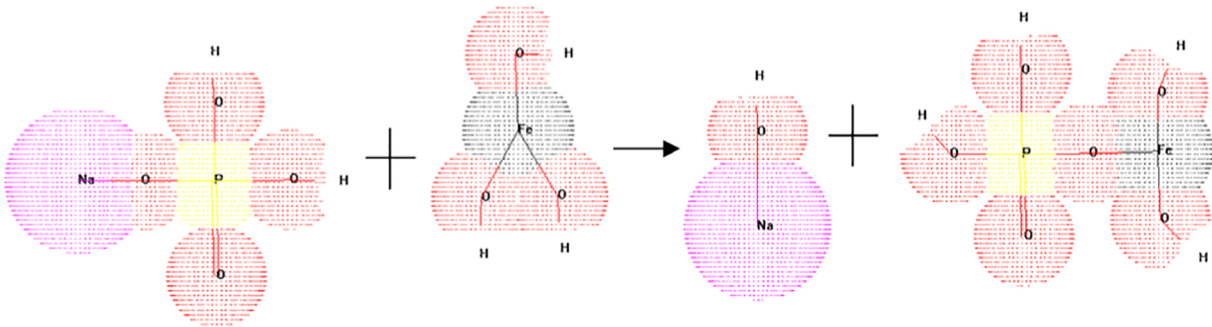


Figure 4

◆ Adsorption ◇ Desorption

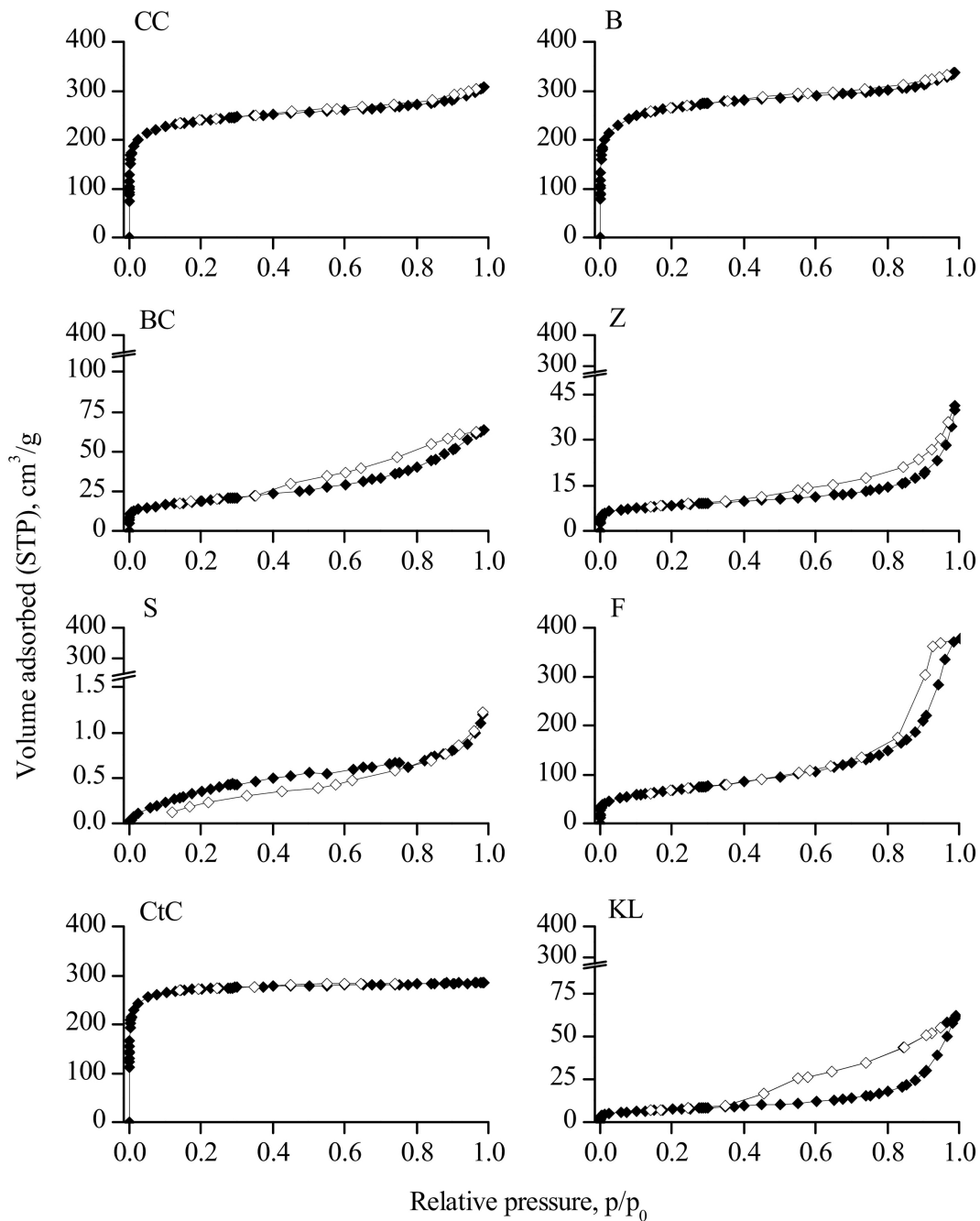


Figure 5

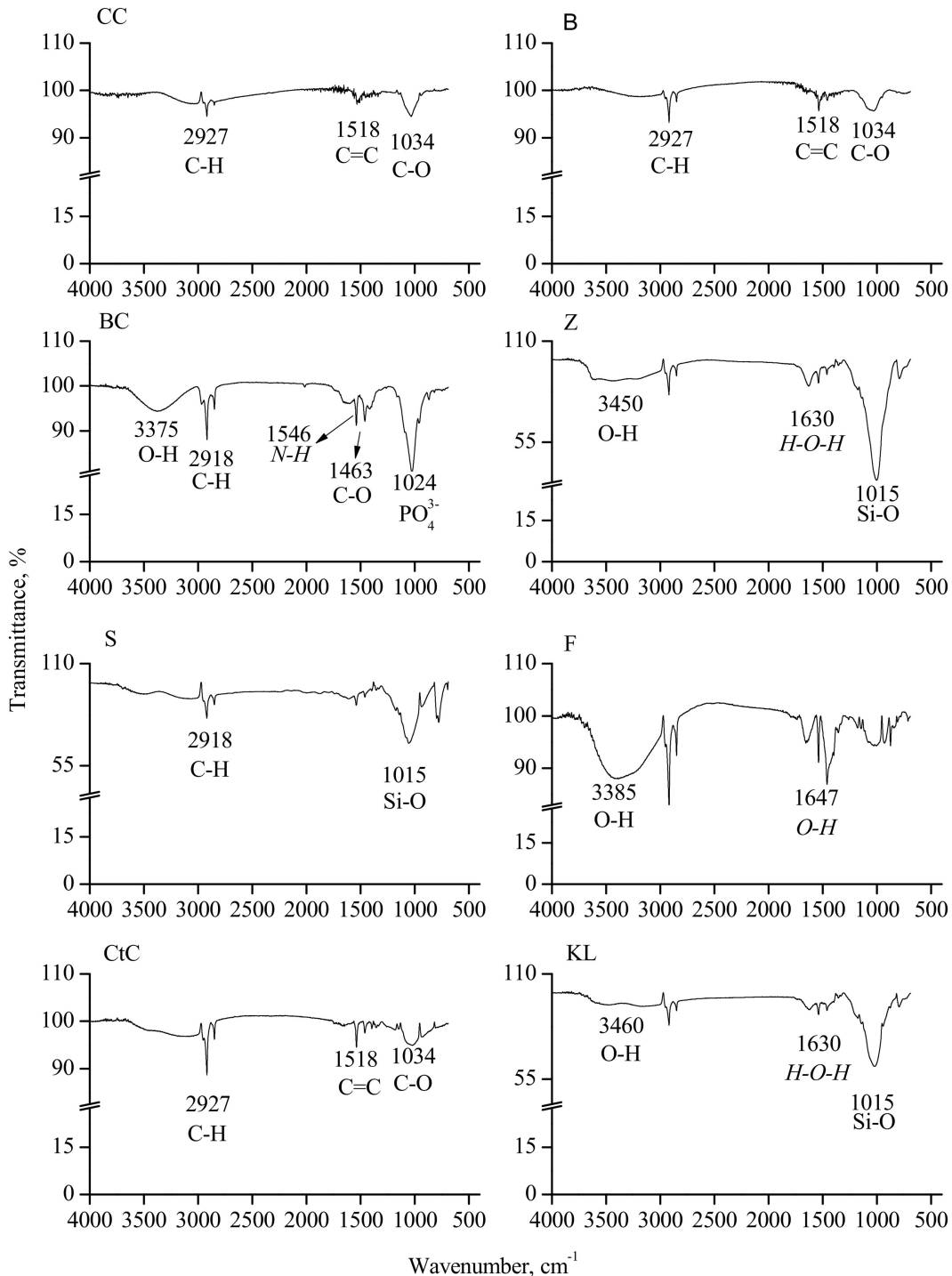


Figure 6

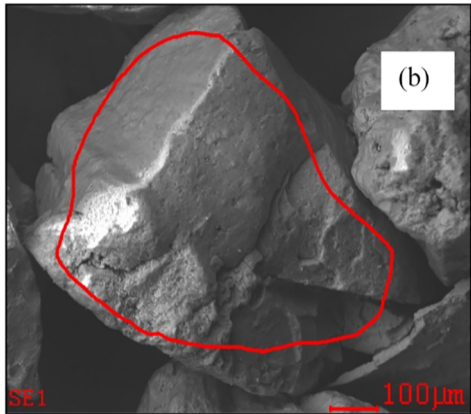
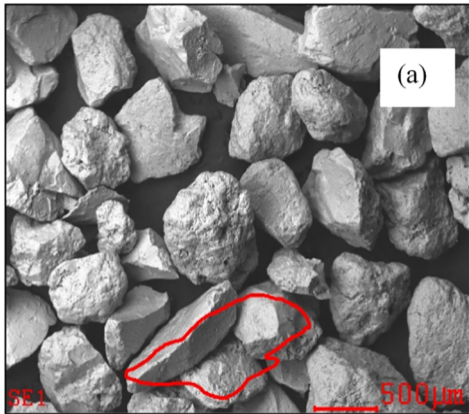


Figure 7

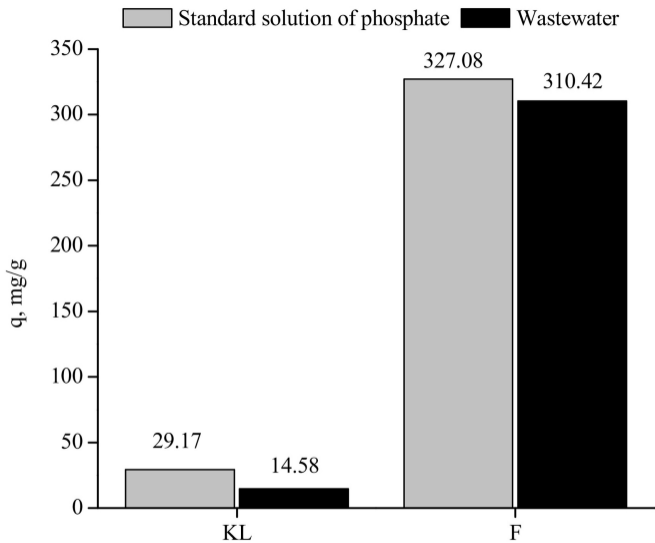


Figure 8